Design of Predistorter Using Measured Nonlinear Characteristics of Power Amplifier with Memory Effect

Yasuyuki Oishi, Shigekazu Kimura, Eisuke Fukuda and Takeshi Takano
Network Systems Laboratories
FUJITSU LABORATORIES LTD.
Kanagawa, Japan

Daisuke Takago, Yoshimasa Daido
Division of Information and Computer Science
Kanazawa Institute of Technology
Ishikawa, Japan

Kiyomichi Araki
Department of Electrical and Electronic Engineering
Tokyo Institute of Technology
Tokyo, Japan

Abstract— **This paper describes a method to design a predistorter (PD) for a power amplifier (PA) with a memory effect by using nonlinear parameters extracted from measured intermodulation distortion (IMD) for a GaN-FET amplifier. To improve the computational efficiency, the updating of a cancellation signal is provided by an iterative algorithm. It is confirmed that the proposed algorithm attains computational intensity lower than half of a memory polynomial. A computer simulation has clarified that the PD improves the adjacent channel leakage power ratio (ACLR) of OFDM signals with several hundred subcarriers corresponding to 4G mobile radio communications. It has been confirmed that a fifth-order PD is effective up to a higher power level. The improvement of error vector magnitude (EVM) by the PD is also simulated for OFDM signals of which the subcarrier channels are modulated by 16 QAM.**

Keywords; power amplifier, IMD, memory effect, predistorter

I. INTRODUCTION

The higher transmission rate of recent mobile communication systems with linear modulation schemes causes a higher peak to average power ratio (PAPR), which imposes more severe requirements on a power amplifier (PA). High efficiency for the PA is also required to reduce the power consumption of the system. A linearization is an inevitable technique to correspond to both of the two mutually contradicting requirements.

Among the existing linearization methods, the most cost-effective method is a predistorter (PD) of which good performance has been reported for applications to second-generation mobile communication systems such as IS-95[1] and CDMA 2000[2]. However, memory effects cannot be neglected according to the increase in the signal bandwidth. Asymmetry in two-tone intermodulation distortion (IMD) has been observed for the PA with the memory effects that degrade the performance of the PD. The memory effects are investigated by using a Volterra series analysis [3]-[6]. These analyses have provided models for thermal and electrical memory effects.

The measurement methods for IMD have been described to confirm the validity of the models [4], [6]. The measurement of an IMD phase requires laborious task in these methods because the IMD sideband is cancelled by inserting a signal with the same amplitude and opposite phase. Our previous papers have described simple and accurate methods to measure the phase and amplitude of IMD [7], [8]. The measured IMDs are fitted by the calculated ones where the bias impedance is assumed to be a parallel RLC circuit, similar to that in [6]. The coincidence of the calculated and measured IMDs is obtained by assuming a model structure for the PA, which is similar to that described by C. Rey et al. [9]; their paper has also suggested a reduction in computational intensity by using IIR-based functions.

This paper describes an extension of the method in [9] to be applicable to the memory effect with a second-order lag. The computational intensity to obtain the cancellation signal of the PD is equivalent to that of a memory polynomial with a memory depth of two.

II. CHARACTERIZATION OF POWER AMPLIFIER USING MEASURED IMD

Figure 1 shows the circuit configuration. A drain bias circuit $F(\omega)$ causes a memory effect by even-order nonlinearies of a power amplifier. Figs. 2 and 3 show the amplitude and phase of IMD, respectively. The solid and dashed curves show the measured and calculated IMDs [8], respectively. A device under target (DUT) is a GaN-FET power amplifier with the carrier frequency of 2 GHz. A coaxial cable with a length of 1.5 m is connected between the drain source and bias supply to enhance the memory effect. The enhancement of the memory effect has two objects: one is to clarify the frequency dependence of IMD, and the other is to confirm the effectiveness of the PD for a long-term memory effect.

A parallel RLC circuit is assumed with bias impedance for the dashed curves because the amplitude of IMD has peaks peculiar to parallel resonance [6]. The coincidence of solid and dashed curves means the validity of the assumption.

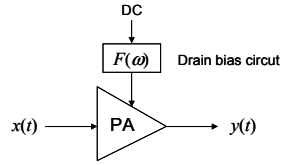

Figure 1. Circuit configuration

978-1-4673-0990-5/12/$31.00 ©2012 IEEE

These figures show the existence of two resonance frequencies: one at 2.4 and the other at 1.2 MHz. The resonance frequency for the bias impedance is 4.8 MHz: the second-order harmonic of the envelope frequency provides peaks at ±2.4 MHz and the fourth-order harmonic provides them at ±1.2 MHz. The mechanism to generate even-order harmonics is given in the model of PA shown in Fig. 4.

The output signal $y(t)$ is given by

$$y(t) = \sum_{m=0}^{2} A_{2m+1}|x(t)|^{2m}x(t) + \sum_{m=1}^{2}\sum_{k=1}^{m} C_{mk}x(t)|x(t)|^{2(m-k)}\int_{-\infty}^{\infty}|x(t-s)|^{2k}f(s)ds \quad (1)$$

where $f(t)$ is the impulse response of the bias impedance $F(\omega)$. The parameter C_{mk} shows a product of coefficients b_{2k} and c_{2n} in Fig. 4.

$$C_{mk} = b_{2k}c_{2(m-k)} \quad (2)$$

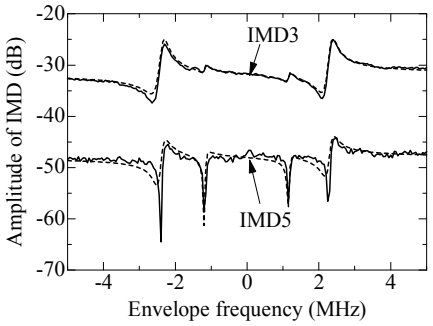

Figure 2. Amplitude of measured IMD for a GaN-FET power amplifier. Solid curves show measured IMD and dashed curves show fitted values, assuming parallel resonance bias impedance.

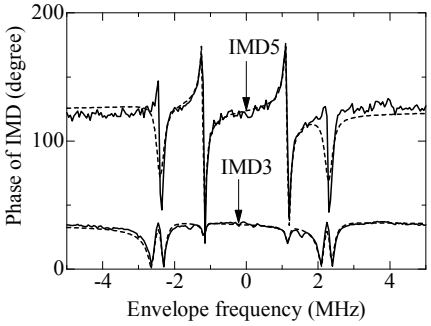

Figure 3. Phase of measured IMD.

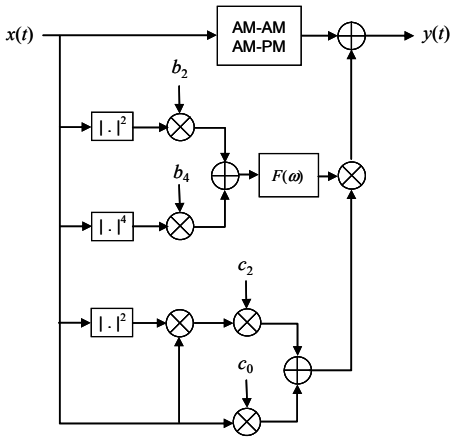

Figure 4. Model of PA consistent with measured IMD.

The parameter A_{2m+1} specifies memory-less nonlinearity causing AM-AM and AM-PM. A two-tone input is assumed to calculate IMD of the PA.

$$x(t) = a\{\exp[j(\omega_c - \omega_e)t] + \exp[j(\omega_c + \omega_e)t]\} = 2a\cos(\omega_e t)\exp(j\omega_c t) \quad (3)$$

where ω_c and ω_e are the center and envelope frequencies. The output $y(t)$ for the two-tone input is obtained by substituting (3) in (1). For parallel resonant circuit, $F(\omega)$ is given by

$$F(\omega) = \frac{j\omega L}{1 - \frac{\omega^2}{\omega_0^2} + j\frac{\omega}{\omega_0}Q} \quad (4)$$

The parameters A_{2m+1}, C_{mk}, Q, and ω_0 are determined to minimize difference between measured and calculated IMD in Figs. 2 and 3 by the least mean square method.

III. Design of Predistorter Based on Measured IMD of PA

The predistorter (PD) is designed by using nonlinear parameters extracted from the measured IMD in the previous section. The concatenated connection of PD and PA is considered as shown in Fig. 5.

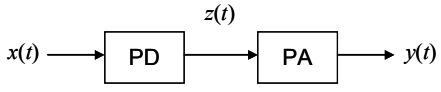

Figure 5. Concatenated connection of PD and PA.

A. Output Signal of Predistorter

Since the output signal $z(t)$ of the PD is fed to the PA, the output signal $y(t)$ is obtained by replacing $x(t)$ in (1) by $z(t)$.

$$y(t) = A_1 z + w_3(z) + w_5(z) \tag{5}$$

where $z(t)$ is written as "z." A function of the nonlinear order of $2m+1$ is given as

$$\begin{aligned} w_{2m+1}(z) &= A_{2m+1}\left|z(t)\right|^{2m} z(t) \\ &+ \sum_{k=1}^{m} C_{mk} z(t)\left|z(t)\right|^{2(m-k)} \int_{-\infty}^{\infty} \left|z(t-s)\right|^{2k} f(s)ds \end{aligned} \tag{6}$$

The output signal $z(t)$ of the PD is assumed to be a sum of the odd-order terms

$$z(t) = x(t) + U_3(t) + U_5(t) \tag{7}$$

The terms $U_3(t)$ and $U_5(t)$ correspond to the third- and fifth-order inverse, respectively. The output signal is rearranged according to the order of nonlinearity and is given by

$$\begin{aligned} y(t) &= A_1 x(t) + [A_1 U_3(t) + w_3(x)] \\ &+ [A_1 U_5(t) + w_{35}(x, U_3) + w_5(x)] + \ldots \end{aligned} \tag{8}$$

where $w_{35}(x, U_3)$ is the fifth-order term generated by $w_3(z)$, i.e.

$$\begin{aligned} w_{35}(x, U_3) &= A_3[2U_3(t)x^*(t) + U_3^*(t)x(t)]x(t) \\ &+ B_{11}\{v_2(t)U_3(t) + x(t)[K_{31}(t) + K_{31}^*(t)]\} \end{aligned} \tag{9}$$

where K_{31} is given by

$$K_{31}(t) = \int_0^t U_3(t-s)x^*(t-s)f(s)ds \tag{10}$$

To cancel the third-order term, $U_3(t)$ is determined as

$$U_3(t) = -\frac{w_3(x)}{A_1} \tag{11}$$

Similarly, $U_5(t)$ is determined as

$$U_5(t) = -\frac{1}{A_1}\left[w_{35}(x, U_3) + w_5(x)\right] \tag{12}$$

The PD cancels lower-order nonlinear distortion in exchange with increase of higher-order distortions. The assumption shown by the following inequality is important to assure that the PD reduces nonlinear distortions as a whole. This inequality is satisfied for most of amplifiers within wide operational output levels.

$$\left|A_1 z(t)\right| \rangle\rangle \left|w_3(z)\right| \rangle\rangle \left|w_5(z)\right| \tag{13}$$

The times for additions and multiplications are estimated, and results are summarized in Table 1, which shows the required calculation times to obtain the output signal of the PD. The calculation times for memory polynomials [11], [12] are estimated to compare with that for this paper. In [11], the memory polynomial model is given by

$$y(n) = \sum_{k=1}^{K}\sum_{q=0}^{Q} b_{kq} x(n-q)\left|x(n-q)\right|^{2(k-1)} \tag{14}$$

where K is an order of nonlinearity and Q is a memory depth. It is shown that the proposed algorithm reduces the computational intensity to lower than half of that required by the memory polynomials.

TABLE I. COMPARISON OF REQUIRED CALCULATION TIME

	Multiplication	Addition
This paper	16	12
K=4, Q=7	40	24
K=9, Q=5	54	40

The required calculation time for this paper is compared to that for a memory polynomial with an order of nonlinearity K and memory depth Q.

IV. PERFORMANCE OF PREDISTORTER

A. Computer Simulation of Output Spectrum for OFDM Signal

It is known that the distribution function of an OFDM signal tends to be a Gaussian for large number of subcarriers. It is widely accepted that several hundreds are enough for the number of subcarriers. In the following calculations, 400 subcarriers are assumed.

Figures 6 to 8 show the output spectrum of the DUT for three different output levels. The assumed oversampling rate corresponds to a frequency range from $-2B$ to $2B$, where B is the bandwidth of the OFDM signal. The output back-off is 13.5, 10.5, and 7.5 dB for Figs. 6, 7, and 8, respectively. Since any peak reduction techniques are not considered, the output level of the PA has the probability to exceed 1 dB gain compression.

The improvement of the spectrum by the PD is also shown in these figures. The fifth-order PD improves the spectrum for all three power levels over the whole frequency range. However, improvement by the third-order PD is limited in the frequency range from $-1.5B$ to $1.5B$, corresponding to the third-order nonlinear distortion. Outside the range, the spectrum deteriorates owing to increase the fifth-order distortion. At a high input level, deterioration by this distortion exceeds the improvement of the third-order PD, as shown in Fig. 8. It has been shown that the fifth-order PD is suitable to improve the output spectrum of the PD.

Table 2 shows the adjacent channel leakage power ratio (ACLR) when the output back-off is 13.5, 10.5, and 7.5 dB. The PD allows the PA to operate with a smaller output back-off to achieve the same ACLR, which improves the PA efficiency. According to Table 2, an ACLR of -52.5 dB is achieved by the fifth-order PD with an OBO of 7.5 dB; meanwhile, an ACLR of -54.2 dB is obtained without the PD and an OBO of 13.5 dB. Assuming that ACLRs seem almost comparable, this result means that an OBO reduction of 6 dB is achieved by the fifth-order PD.

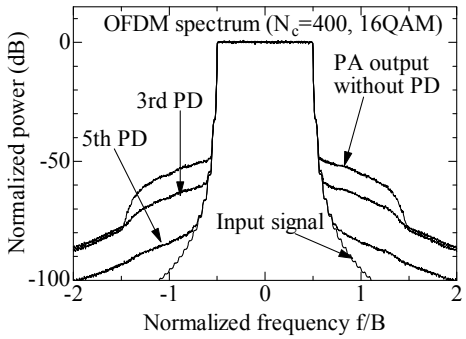

Figure 6. Output spectrum of PA for OFDM signal for lower input level. Output back-off is 13.5 dB. Four times oversampling is assumed to correspond to frequency range from $-2B$ to $2B$, where B is bandwidth of OFDM signal.

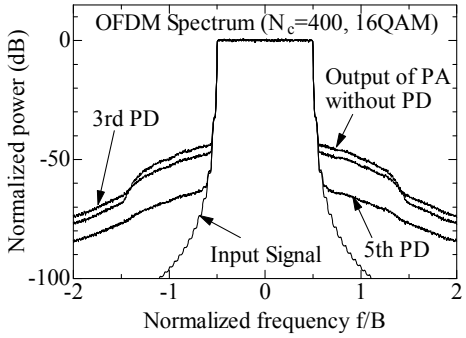

Figure 7. Output spectrum of PA for OFDM signal when output back-off is 10.5 dB.

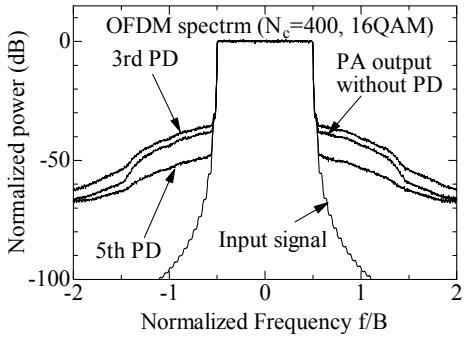

Figure 8. Output spectrum of PA for OFDM signal when output back-off is 7.5 dB.

TABLE II. THE ACLR PROPERTIES WITH/WITHOUT THE PD

(dB)

	Output back-off		
	13.5 dB	10.5 dB	7.5 dB
Without PD	-54.2	-48.5	-42.6
3rd order PD	-63.8	-51.8	-39.8
5th order PD	-75.1	-66.2	-52.5

The ACLR is defined as a power ratio of the adjacent channel to the main channel. The channel separation is B and each bandwidth for power summation is 0.8 B in order to eliminate the effect of OFDM side lobes.

B. Dynamic Behavior of PA and Improvement by PD

There is no one-to-one relation between the input and output signal of the PA with the memory effect owing to the influence of previous input values. Thus, the plural values of the output amplitude and phase correspond to a single value of the input. It is important to know the average and variation range of the output values.

Figure 9 shows the average gain for the PA with and without the PD. The simulated results are compared to the case of the memory-less PA. It is shown in this figure that gain saturation occurs at lower power levels for the PA with the memory effect than the memory-less PA; compare the curve labeled as "AM-AM" to that as "without PD." It is also shown that the third-order PD improves the average gain at a lower input level. However, its performance degrades with an increase in the input level. For the fifth-order PD, the average gain is improved by up to 1 dB compression level.

Figure 10 shows the average phase shift for the PA with and without the PD. The curve indicated as "AM-PM" is calculated for the memory-less PA. The shift of the curve "without PD" is also caused by the memory effect. The third-order PD prevents the phase shift at lower input levels, similar to the case of Fig. 9. The fifth-order PD provides much better performance than the third-order PD, similar to the previous figure.

Figure 11 shows the RMS variation of the output signal. The PA without the PD has RMS variation even at very low input levels. The third-order PD reduces the RMS variation at lower input levels. Its improvement disappears at a level lower by 3.5 dB than 1 dB compression owing to the increase in the fifth-order distortion. The performance of the fifth-order PD is much better and the RMS variation is reduced at all power levels up to 1 dB compression. The RMS variation is equivalent to the error vector magnitude (EVM).

The performance shown in Figs. 9 to 11 assures that the PD works well to cancel the nonlinear distortions of the PA with the memory effect. The dependence of its improvement on the power level coincides that of the power spectra shown in Figs. 6, 7, and 8.

V. CONCLUSION

This paper has described the measured two-tone IMD of a GaN-FET amplifier of which the envelope frequency dependence has peaks peculiar to an RLC parallel resonant

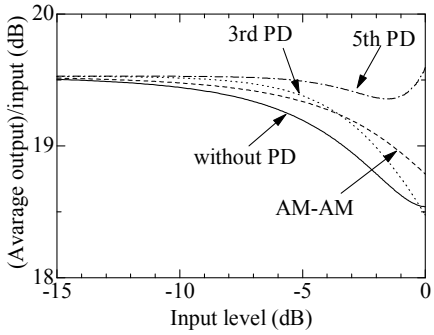

Figure 9. Average gain of PA. Horizontal axis is normalized by the input level corresponding to 1 dB gain compression

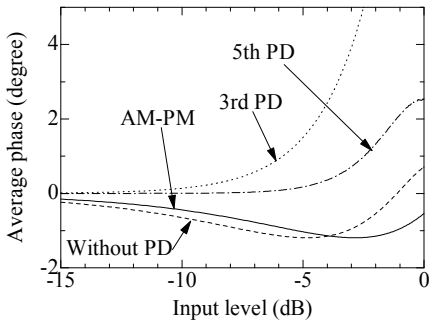

Figure 10. Average output phase shift of PA.

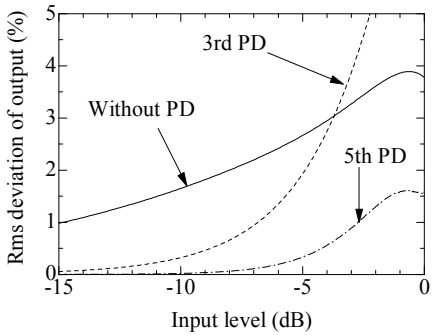

Figure 11. RMS variation output signal of PA.

circuit. The parallel resonant circuit is assumed as bias impedance used in a model structure to explain the nonlinear behavior of the amplifier. The calculated amplitude and phase of IMD using the model have coincided with the measured ones when optimization is made for the nonlinear coefficients of the PA and parameters of the bias impedance. These optimized parameters are used to determine the third- and fifth-order inverses of the amplifier.

Computational intensities for updating the inverse have been reduced by an algorithm that uses a similar idea to the polynomials of IIR-based functions. An existing method attains computational intensity equivalent to a memory depth of two for the memory effect with a first-order lag. The described algorithm extends the method to attain an equivalent memory depth of two for the memory effect with a second-order lag. The required times for additions and multiplications by the algorithm have been compared to that for a memory polynomial. It has been shown that the algorithm reduces the computational intensity to lower than half of that required by the memory polynomials.

Using the algorithm, the output spectrum of the PA is estimated for OFDM signals with 400 subcarriers, each of which is modulated by 16 QAM. It has been confirmed that the fifth-order PD improves the spectrum for all three simulated power levels.

A computer simulation has also been made to estimate the error vector magnitude (EVM) of the PA. The results show that the fifth-order PD is effective to reduce EVM.

REFERENCES

[1] S. Kusunoki, K. Yamamoto, T. Hatsugai, H. Nagaoka, K. Tagami, N. Tominaga, K. Osawa. K.Tanabe, S. Sakurai, and T. Iida, "Power-amplifier module with digital adaptive predistortion for cellular phones," IEEE Trans. Microwave Theory Tech. vol. 50, no. 12, pp.2979-2986, Dec. 2002

[2] S. Boumaiza, and F. M. Ghannouchi, "Realistic power-amplifiers characterization with application to baseband digital predistortion for 3G base stations," IEEE Trans. Microwave Theory Tech. vol. 50, no.12, pp.3016-3021, Dec. 2002

[3] J. Vuolevi, J. Manninen, and T. Rahkonen, "Memory effect compensation in RF power amplifiers by using envelope injection technique," IEEE Radio and Wireless Conference 2001, Rec. pp. 257-260, Aug. 2001.

[4] J. Vuolevi, J. Manninen, and T. Rahkonen, "Measurement technique for characterizing memory effects in RF power amplifiers," IEEE Trans. Microwave Theory Tech. vol. 49, no.8, pp.1383-1389, August, 2001

[5] N. B. Carvalho, and J. C. Pedro, "A Comprehensive explanation of distortion sideband asymmetry," IEEE Trans. Microwave Theory Tech. vol. 50, no. 9, pp.2090-2101, Sept. 2002.

[6] J. S. Kenney and P. Fedorenko, "Identification of RF power amplifier memory effect origins using third-order intermodulation distortion amplitude and phase asymmetry," Microwave Symposium Digest, 2006, IEEE MTT-S International, pp.1121-1124, June 2006.

[7] T. Takano, Y. Ohishi, S. Kimura, M. Nakamura, K. Nagatani, E. Fukuda, Y. Daido, K. Araki, "Efficient Method to Measure IMD of Power Amplifier with Simplified Phase Determination Procedure to Clarify Memory Effects Origin," IEICE Trans. on Electron. vol. E93-C, no.7, pp. 991-999, July 2010.

[8] Y. Oishi, S. Kimura, E. Funkuda, T. Takano, Y. Daido, and K. Araki, "Iterative determination of phase reference in IMD measurement to characterize nonlinear behaviour, and to derive inverse, for power amplifier with memory effect," IEICE Trans. on Electron. vol. E94-C, no. 10, pp. 1515-1523, Oct. 2011.

[9] C. Rey, M. Masood, J. Staudinger, and. S. Kenney, "RF power amplifier modeling using polynomials with IIR bases functions," IEEE Radio and Wireless Symposium pp. 43-46, Jan. 2009.

[10] K. A. I. L. W. Gamalath, "Introduction to Fourier transforms in physics," Foudation Books, Cambridge Univ. Press India Pvt. Ltd. 2007, ISBN: 978-81-7596-434-1, pp.83-84, 2007.

[11] H. Zhou, G. Wan, and L. Chen, "A nonlinear memory power amplifier behavior modeling and identification based on memory polynomial model in soft-defined shortwave transmitter," Wireless Communications Networking and Mobile Computing (WiCOM), 2010 6th International Conf. pp. 1-4, Sept. 2010.

[12] C. Yu, Y. Liu, and S. Li, "Adaptive order-decision method for memory polynomial based predistorters," Wireless Communications Networking and Mobile Computing (WiCOM), 2009 5th International Conf. pp. 1-4, Sept. 2009.